

The Baghdad Atlas: A relational database of inelastic neutron-scattering $(n, n'\gamma)$ data

A. M. Hurst^{a,*}, L. A. Bernstein^{a,b}, K. Song^a

^a*Department of Nuclear Engineering, University of California, Berkeley, California 94720, USA*

^b*Lawrence Berkeley National Laboratory, Berkeley, California 94720, USA*

Abstract

A relational database has been developed based on the original $(n, n'\gamma)$ work carried out by A. M. Demidov *et al.*, at the Nuclear Research Institute in Baghdad, Iraq [“Atlas of Gamma-Ray Spectra from the Inelastic Scattering of Reactor Fast Neutrons”, Nuclear Research Institute, Baghdad, Iraq (Moscow, Atomizdat 1978)] for 105 independent measurements comprising 76 elemental samples of natural composition and 29 isotopically-enriched samples. The information from this Atlas includes: γ -ray energies and intensities; nuclide and level data corresponding to the residual nucleus and meta data associated with the target sample that allows for the extraction of the flux-weighted $(n, n'\gamma)$ cross sections for a given transition relative to a defined value. The fast-neutron flux-weighted partial γ -ray cross section from ENDF/B-VIII.0 for the production of the 846.8-keV $2_1^+ \rightarrow 0_{gs}^+$ transition in ^{56}Fe , $\sigma_\gamma = 329.46 \pm 37.55$ mb, is used for this purpose. This result takes into account contributions from the β^- decay of ^{56}Mn formed in the $^{56}\text{Fe}(n, p)$ reaction. However, different values for the adopted cross section can be readily implemented to accommodate user preference based on revised determinations of this quantity. The Atlas $(n, n'\gamma)$ data has been compiled into a series of CSV-style ASCII data sets and a suite of Python scripts have been developed to build and install the database locally. The database can then be accessed directly through the SQLite engine, or using alternative methods such as the Jupyter Notebook Python-browser interface. Several examples exploiting different interaction methodologies are distributed with the complete software package.

Keywords: Inelastic neutron scattering γ -ray data, partial γ -ray cross sections, relational database.

1. Introduction

Inelastic neutron scattering is a dominant energy-loss mechanism for fast neutrons in heavy ($A > 12$) nuclei and produces unique γ -ray signatures of the material which the neutrons are incident upon. As such, a good knowledge of it is required for virtually all branches of applied nuclear science ranging from shielding calculations to the design of ad-

vanced nuclear-energy systems to international security and counter proliferation. The need for improved neutron-scattering data was explicitly stated in a number of recent nuclear data workshops, including the white papers from the Nuclear Data Needs and Capabilities for Applications Workshop [1], the Nuclear Data Roadmapping Enhancement Workshop in 2018 [2] and the Workshop for Applied Nuclear Data Activities in 2019 [3]. In addition to its utility for nuclear applications, $(n, n'\gamma)$ data provides unique insight into off-yrast nuclear structure due to the non-selective nature of the reaction (which can

*Corresponding author.

Email address: amhurst@berkeley.edu (A. M. Hurst)

URL: <http://nucldata.berkeley.edu> (A. M. Hurst)

include a significant compound component) and the wide range of angular momentum states accessible to fast neutrons.

Angle-differential (n, n') data is challenging to measure due to the difficulties involved in measuring the neutron energy and large backgrounds from elastic scattering. An alternate approach to determining $(n, n'\gamma)$ cross sections involves measuring the prompt γ rays emitted from the excited states populated via inelastic scattering. While these measurements lack the angle-differential information needed to help improve neutron transport, they can provide an important integral constraint to the nuclear-reaction evaluation process and can be used to improve modeling for non-destructive assay of materials using active-neutron interrogation.

Unfortunately, there are no modern compilations of inelastic-scattering γ -ray production cross sections. This is in part due to a fundamental lack of data, but also to the fact that since $(n, n'\gamma)$ includes both discrete γ -ray transition and cross section data it does not fit well into either of the two main compilation databases: Experimental Nuclear Reaction Data (EXFOR) [4] for reactions, and Experimental Un-evaluated Nuclear Data List (XUNDL) [5] for structure. The “*Atlas of Gamma-rays from the Inelastic Scattering of Reactor Fast Neutrons*” published by A. M. Demidov *et al.*, [6] is one of the most comprehensive compilations of data on $(n, n'\gamma)$ in existence containing 7375 γ rays (of these, 6870 represent firm assignments, while 505 are tentative) from 76 natural and 29 isotopically-enriched targets, measured at the IRT-5000 Reactor at the Nuclear Research Institute, near Baghdad, Iraq. Until recently this information has only been available in its [out-of-print] book format. To enhance the utility of this Atlas and increase its accessibility to the international community, we have compiled the data into a set of CSV-style ASCII tables and developed software to build the corresponding SQLite (structured query language) database locally. The software package is disseminated online through the Berkeley Nuclear Data Group [7] and the National Nuclear Data Center (NNDC) [8]. This paper describes how the data were originally obtained along with query-based methods for extraction of absolute partial γ -ray pro-

duction cross sections from the reported [6] relative-intensity data.

2. Inelastic-scattering $(n, n'\gamma)$ data

The data in the “Baghdad Atlas” [6] comes from a single lithium-drifted germanium [Ge(Li)] γ -ray detector oriented perpendicular to a filtered “fast” neutron beam line at the IRT-5000 reactor, formerly located at the Al-Tuwaittha Nuclear Research Institute outside of Baghdad, Iraq. While the details of the neutron spectrum are not completely known, the experimental setup was designed to minimize the presence of low-energy thermal neutrons. Their success is evident in that there are only 30 transitions throughout the entire Atlas known to arise from radiative-capture (n, γ) reactions. In this paper we only provide sufficient details of the neutron flux and spectroscopy measurements necessary to determine cross sections on an absolute scale for all data contained in the Atlas. The experimental setup used at the Baghdad reactor is described in greater detail in Refs. [9, 10].

2.1. Neutron flux

The neutron spectrum is characterized as having a monotonically-decreasing flux (ϕ) with increasing neutron energy (E_n), ranging from approximately 0.5 – 10 MeV as shown in Fig. 1, where the measured IRT-5000 data is taken from Refs. [6, 9]. The flux-average neutron energy for this spectrum is determined to be $\langle E_n \rangle = 1.17$ MeV. To a first approximation, the authors of the Atlas suggest the reactor neutron spectrum at $E_n > 1.0$ MeV falls off according to the exponential-attenuation law of the form:

$$\phi(E_n) \propto \exp(-\beta E_n), \quad (1)$$

where $\beta = 0.7$ [6]. However, in a previous interpretation of the same measured spectrum, the authors suggest the flux may be approximated in accordance with $\exp(-0.72E_n)$: $\forall E_n > 1.5$ MeV [9]. In earlier work still, it is noted that this exponent may, in fact, vary from approximately $\beta \approx 0.65 - 0.75$ [11] depending on the reactor type. However, the relative γ -ray intensities corresponding to transitions

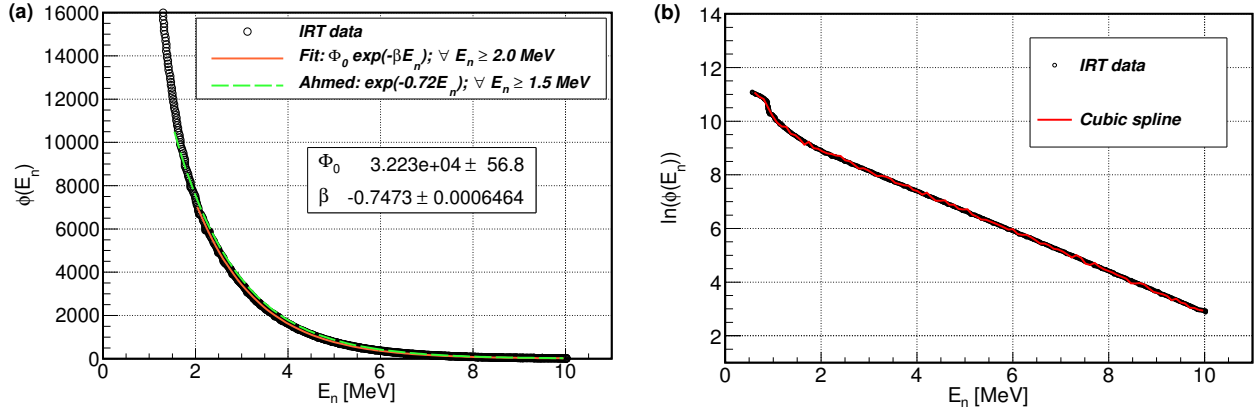


Figure 1: The IRT-5000 Baghdad reactor neutron flux shown as a function of neutron energy. The data are taken from Ref. [6] and correspond to the fast-neutron spectrum of the water-cooled water-moderated reactor after filtration of the beam through a 10.1-cm layer comprising lead (9 cm), boron carbide (1 cm) and cadmium (1 mm). The fit in (a) corresponds to an exponential of the form $\exp(-\beta E_n)$ [solid-orange curve], where $\beta = 0.7473$ and $\phi_0 = 32230$ are determined from a fit to the data for $E_n \geq 2$ MeV. An exponential of the form $\exp(-0.72 E_n)$ [9] is also drawn for comparison (dashed-green curve); to obtain this function we fixed the value of β to 0.72 and ϕ_0 was treated as a free parameter determined in an independent fit corresponding to $E_n \geq 1.5$ MeV. The same flux spectrum plotted in \log_E -space is shown in (b) illustrating a cubic-spline fit used for interpolation.

from levels above 0.5 MeV are not expected to be strongly affected by different values of β [6]. Because the observed $(n, n'\gamma)$ spectra from reactor fast neutrons are largely influenced by the increasing nuclear level density with increasing atomic mass A (away from closed shells), the γ -ray intensity data presented in the Baghdad Atlas can be expected to be universal for fission-based neutron sources [6].

In our attempts to fit the IRT-5000 reactor flux data from Ref. [6] with a single exponential of the form given by Eq. (1), we have determined a value of $\beta = 0.7473$ corresponding to the energy region $E_n > 2.0$ MeV, as shown by the fit in Fig. 1(a). Our value of β is appreciably larger (approximately 3.8 – 6.8%) than the values reported in Refs. [6, 9], but falls within the expected range defined in Ref. [11]. At lower neutron energies the authors suggest that a more complicated function is needed to describe the behaviour of the neutron flux. This is evident from Fig. 1(a) where simple exponentials (assuming values of $\beta = 0.72$ [9] and $\beta = 0.7473$) are inadequate at reproducing the reported flux. Because of the uncertainty in the low-energy behaviour, we have used a cubic-spline interpolation method [Fig. 1(b)] to de-

scribe the overall flux distribution, where the continuous exponential functions are asymptotic with the spline-interpolated results in the neutron-energy region $E_n > 2.0$ MeV.

2.2. γ -ray spectrometry

All of the data in the Atlas were acquired under identical conditions using the same experimental configuration with a single Ge(Li) γ -ray detector oriented at 90° to the neutron beam line, with samples positioned at 60° relative to the incident neutron beam in a 25×25 mm² holder [9]. A beam-spot diameter of ~ 30 mm was achieved at the target position [6] and spectra were collected for neutron irradiation periods ranging from 3 – 44 h [6]. The irradiated samples varied in mass from 1 g (Eu₂O₃) to 125 g (Hg). For measurements of most elements and enriched isotopes, a 30 cm³ Ge(Li) detector with an energy resolution of 3.8 keV at 1.2 MeV [6, 9] was used. A 40 cm³ Ge(Li) detector with an energy resolution of 2 keV at 1.2 MeV [6] was also used for the elemental-sample measurements of chlorine, scandium, bromine, lutetium, osmium, and iridium, along with the isotopes of tellurium.

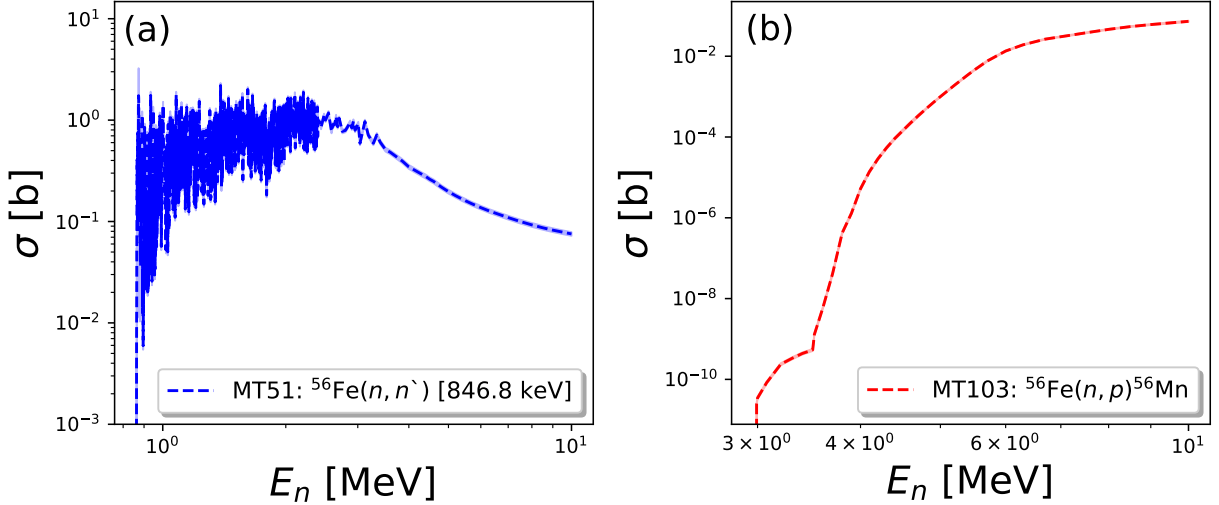


Figure 2: Cross-section data taken from the ENDF/B-VIII.0 [12] library for (a) the $^{56}\text{Fe}(n, n')$ reaction corresponding to the first excited 2^+ state at 846.8 keV (MT51 sub-library; blue-dashed curve), and (b) the excitation function for the $^{56}\text{Fe}(n, p)^{56}\text{Mn}$ reaction (MT103 sub-library; red-dashed curve). The shaded region on each plot corresponds to the uncertainty band.

For each measurement, the Ge(Li) detector was isolated from the fast-neutron flux by surrounding it with shielding materials comprised of a 5-cm thick iron plate, an 8-cm layer of paraffin mixed with boron carbide (B_4C), and a 10-cm thick lead plate. A 20-mm diameter by 110-mm length LiH layer with a density of 0.53 g/cm^3 [9] was also placed into a collimating channel of the shielding material to filter γ rays originating within the target from fast neutrons scattered by the sample itself.

Energy and efficiency calibrations of the Ge(Li) detectors were performed using a variety of standard radioactive (^{75}Se , ^{182}Ta , ^{110}Ag , ^{72}Ga , ^{140}La , ^{24}Na , and ^{134}Cs) and reaction [$^{28}\text{Si}(n, \gamma)^{29}\text{Si}$] sources for energies below and above 3 MeV, respectively. All γ -ray intensities (I_γ) were measured at 90° relative to the neutron beam line and were corrected for self-absorption effects in the sample. The measured γ -ray energies (E_γ) are reported in the Baghdad Atlas [6] together with uncertainties due to calibration and non-linearity of the spectroscopic tract for E_γ . The associated uncertainties for the I_γ measurements listed in the Atlas include statistical contributions

(with 95% probability) together with uncertainties due to detector-efficiency determination and γ -ray self absorption.

The γ -ray transition intensities for all elements and enriched isotopes reported in the Atlas are presented in comparison to the 846.8-keV transition in ^{56}Fe [13], corresponding to the $2_1^+ \rightarrow 0_{\text{gs}}^+$ transition observed in the $^{56}\text{Fe}(n, n'\gamma)$ reaction. The relative intensity of the 846.8-keV line is defined to be 100% [6]. This provides a unique normalization reference point for all other elements (or enriched isotopes) since a reliable γ -ray transition belonging to each element (enriched isotope) was measured relative to the ^{56}Fe 846.8-keV γ line. All other γ lines from each respective elemental [enriched isotope] ($n, n'\gamma$) measurement were then measured and reported relative to the selected elemental (enriched-isotope) normalization γ ray; these normalization γ -ray lines, together with their ^{56}Fe -relative-intensity values, are tabulated in [Table 2 of] the Baghdad Atlas [6].

3. Cross-section calculations

The γ -ray intensities reported in the Baghdad Atlas [6] have all been deduced using the two-stage normalization procedure described in Sect. 2.2. This method allows for all $I_\gamma(90^\circ)$ values to be presented on an absolute scale relative to an assumed absolute intensity, or cross section, for the 846.8-keV $2_1^+ \rightarrow 0_{\text{gs}}^+$ transition in the $^{56}\text{Fe}(n, n'\gamma)$ reaction. We have therefore deduced a value for the flux-weighted cross section for this transition, $\langle\sigma_{\gamma 847}\rangle$, to permit for the determination of partial γ -ray production cross sections for all Atlas-reported $I_\gamma(90^\circ)$ data [6]. This expectation value can be determined by convolving the neutron flux spectrum shown in Fig. 1 with the (n, n') cross-section data shown in Fig. 2(a) that are taken from the Evaluated Nuclear Data File library, ENDF/B-VIII.0 [12], to first obtain the production cross section for the 2_1^+ state from the (n, n') channel according to the expression

$$\langle\sigma_{nn}(2_1^+)\rangle = R \cdot \frac{\int_0^{E_n=10} \phi(E_n) \sigma_{nn}(E_n) dE_n}{\int_0^{E_n=10} \phi(E_n) dE_n}. \quad (2)$$

Here, $R = 1$ (i.e., 100%) is the branching ratio of the 846.8-keV γ ray that deexcites the 846.8-keV 2_1^+ level in ^{56}Fe as reported in the Evaluated Nuclear Structure Data File (ENSDF) for ^{56}Fe [13], and $\phi(E_n)$ is the measured reactor neutron flux [6, 9] at incident neutron energy E_n . The ENDF/B-VIII.0 neutron-energy dependent excitation function $[\sigma_{nn}(E_n)]$ for the 2_1^+ state (sub-library MT51 [12]) in ^{56}Fe corresponds to both direct population of the level itself and indirect feeding from higher-lying levels, accounting for both the direct-production and compound-nucleus formation processes involved in the inelastic neutron-scattering reaction channel.

Because the cross-section data in ENDF/B-VIII.0 are discretized according to E_n , we may recast Eq. (2) as a summation over the observed flux spectrum at

the specified neutron-energy intervals as

$$\langle\sigma_{nn}(2_1^+)\rangle = R \cdot \frac{\sum_{k=0}^N \phi_k(E_n) \sigma_{nn,k}(E_n) \Delta E_n}{\sum_{k=0}^N \phi_k(E_n) \Delta E_n}, \quad (3)$$

where the summation goes from the excited-state production threshold ($k = 0$) up to 10 MeV [cf. the integration limits in Eq. (2)] and N represents the degree of neutron-energy/cross-section discretization of the ENDF/B-VIII.0 sub-library over the corresponding incident-neutron-energy interval. In Eq. (3), above, $\phi(E_n)$ values are interpolated from the measured spectrum in Fig. 1 according to the N -discretized values of E_n using the cubic-spline method described in Sect. 2.1 [see Fig. 1(b)]. Using this approach, we find an overall expectation value $\langle\sigma_{nn}(2_1^+)\rangle = 330.37$ mb for the production of the 2_1^+ state in ^{56}Fe , and similarly, we establish a flux-weighted uncertainty of ± 37.55 mb from the associated covariances in the corresponding ENDF-B/VIII.0 library [12].

There is, however, an additional contribution to the 846.8-keV transition which can be attributed to the β^- decay of ^{56}Mn formed in the $^{56}\text{Fe}(n, p)$ reaction, which subsequently populates the 846.8-keV level in ^{56}Fe with a 98.85(3)% branching ratio [13]. This contribution can be calculated using the same flux-weighted approach given by Eqs. (2) and (3), where σ_{nn} is replaced for σ_{np} , because the experiment was performed over a relatively long period of time (8 h) compared to the lifetime of ^{56}Mn ($t_{1/2} \approx 2.6$ h [13]), allowing it to come into secular equilibrium. We have estimated this contribution using the ENDF/B-VIII.0 cross-section library (MF3) for the $^{56}\text{Fe}(n, p)$ reaction (sub-library MT103 [12]), illustrated in Fig. 2(b), to arrive at a small correction of $\langle\sigma_{np}(2_1^+)\rangle = 0.9161 \pm 0.0232$ mb, approximately 0.28% of the (n, n') excitation function for the first 2^+ state in ^{56}Fe . The deduced 2.53% uncertainty in $\langle\sigma_{np}(2_1^+)\rangle$ is dominated by the covariances associated with the relevant ENDF-B/VIII.0 library [12], while the contribution from the measured branching ratio [13] has only a negligible contribution at the $\sim 0.03\%$ level in the overall error budget. Taking this β^- -decay correction factor into account, we ob-

tain a spectrum-averaged, decay-corrected value for $\langle\sigma_{\gamma 847}\rangle$ assuming:

$$\langle\sigma_{\gamma 847}\rangle = \langle\sigma_{nn}(2_1^+)\rangle - \langle\sigma_{np}(2_1^+)\rangle, \quad (4)$$

to arrive at a final adopted cross section $\langle\sigma_{\gamma 847}\rangle = 329.46 \pm 37.55$ mb.

4. Database scope and structure

The data in the Baghdad Atlas is valuable for many applications ranging from nuclear non-proliferation, active neutron-interrogation studies and benchmarking nuclear-reaction models in the fast-fission neutron-energy region. However, its use is limited by the fact that the data was only available in printed form [6]. To enhance its utility we have compiled the data into a set of CSV-style ASCII tables and developed software to produce a locally-installed SQLite relational database. This allows for far greater dissemination, increasing the database accessibility for the international community. The complete package may be downloaded [7, 8] and contains the following components:

- Scripts to compile the data into a SQLite database for both Python 2 and Python 3. The **Makefile** provided will test for the appropriate version and run with the necessary settings.
- Open-source C-code to produce the shared-object dynamic extension-functions library allowing for enhanced functionality in SQL transactions that are not part of the standard SQLite3 library. This library will then provide the user with access to common mathematical (e.g., **cos**, **sin**, **tan**, **exp**, **log**, **log10**, **sqrt**, **pi**, etc.), string (e.g., **replicate**, **replace**, **reverse**, etc.), and aggregate (e.g., **variance**, **mode**, **median**, etc.) functions in SQL queries using the OS libraries or provided definitions. The **Makefile** will establish the correct OS-kernel name and compile the library accordingly.
- The complete set of CSV-style ASCII data files compiled for 76 different elements in the range

$3 \leq Z \leq 92$. This includes data sets from 76 natural samples and 29 isotopically-enriched samples (105 data sets in total).

- A Jupyter Notebook illustrating Python-based methods for interacting with and visualizing the data.
- Several SQL scripts based on standard SQL-transaction methods exemplifying database interaction. The compiled OS-dependent extension-functions library will be initialized as appropriate where required during the build process.
- A PDF of the Baghdad Atlas [6] provided for reference.
- An HTML manual describing the software-installation procedure and data-retrieval methods. An overview of the Baghdad Atlas data is also provided with this documentation. This HTML manual is also available online [7].

4.1. Database schema

The data structure for the $(n, n'\gamma)$ data is described using two relational tables in an SQL schema: **nucleus** and **sample**. The **nucleus** table represents the nuclear-structure type class of information including: chemical symbol and atomic number along with flags to indicate element or enriched isotope identification, γ -ray energies and intensities together with their associated uncertainties, excitation energies of the states populated, and residual-nucleus reaction products. Associated properties of the aforementioned quantities are also contained in this table. The **sample** table contains all meta-data associated with the irradiated sample including: element/isotope identification properties, atomic number, mass number, irradiation exposure period, chemical composition, mass and enrichment data. Normalization γ -ray properties (energies, scaling factors and uncertainties) are also listed in this table. A detailed explanation of the schema is available in the supporting documentation [7].

```

sqlite> SELECT symbol AS "chemical symbol", Z AS "atomic number",
...> sample composition AS "sample composition", mass AS "mass [g]",
...> exposure time AS "exposure time [h]"
...> FROM sample
...> WHERE Z >= 30 AND Z <= 40;
chemical symbol  atomic number  sample composition  mass [g]  exposure time [h]
-----
Zn              30              Zn              31.5      6.0
Ga              31              Ga              15.5      23.0
Ge              32              Ge              4.7       44.0
As              33              As              22.1      21.0
Se              34              Se              24.0      12.9
Br              35              BrInGlass       32.0      12.0
Rb              37              Rb2CO3          15.5      23.0
Sr              38              SrCO3           12.1      9.0
Y               39              Y NO3_3_6H2O    28.9      22.0
Zr              40              ZrO2            42.0      16.1
sqlite>

```

Figure 3: Example of a SQLite transaction using conditional arguments to access information in the Baghdad Atlas database. See text for details.

4.2. Additional requirements

The software provided with this package is intended to create a SQLite database on Linux and Mac OS X platforms. Additional system requirements needed to build the database and run this software include: the SQLite3 database engine [14]; the GNU C compiler [15]; Python 2.7 or Python 3 [16]. In addition, for users that choose to run the provided Jupyter Notebook “as is” will require installation of several third-party Python libraries. These requirements along with other recommendations are outlined in the supporting online documentation [7].

5. Database-retrieval methods

Since we provide access to the source data itself, together with descriptive documentation, this allows users the freedom to parse and manipulate the data sets according to individual needs. However, the database utility and associated software described in this paper offers users a readily-accessible and convenient means for interacting with and visualizing the data. Once built and installed to the appropriate location, database queries can be performed by invoking transactions based on the SQLite syntax. This provides users with a variety of options for retrieving customized data sets based on conditional arguments.

5.1. Terminal command line

The SQLite engine [14] is an embedded SQL database engine providing a terminal-based frontend to the SQLite library that is able to evaluate queries

interactively and display the corresponding results. This method is particularly useful for rapid evaluation of simple queries. Figure 3 illustrates this concept using the SQLite “interpreter” to query the Baghdad Atlas database and retrieve *chemical symbol*, *atomic number*, *sample composition*, *mass*, and *exposure time* information for selective entries from the **sample** relational table that satisfy the atomic number condition: $30 \leq Z \leq 40$. Alternatively, more complicated queries are better handled by reading in scripts, either through the interpreter or, because the SQLite engine also supports batch-mode processing, directly via the command line. Additionally, for users that prefer to interact with the database through a graphical user interface, a variety of open-source cross-platform distributions are available, e.g., Refs. [17], [18]. Several SQL scripts illustrating database interaction and suitable for processing using the aforementioned methods are bundled with the software package.

5.2. Jupyter Notebook

The Jupyter Notebook [19] provides users with a browser-based frontend interface to interact with the SQLite libraries. One of the main advantages of creating Jupyter Notebook projects is that it greatly enhances and facilitates project sharing among researchers, allowing users to create collaborative and reproducible narratives. Although this method requires additional Python-code overhead, it provides a convenient means for populating arrays and lists of data that can be sorted and filtered according to specific requirements. Also, the Jupyter Notebook provides access to a wide range of other useful libraries allowing for implementation of high-level methods to augment the analysis of the data, as well as a high degree of flexibility in displaying the results—including inline visualization of the data for on-the-fly inspection.

Many nuclear data applications require information regarding absolute partial γ -ray cross sections. In recognition of this need, the Notebook bundled with this software package has been developed with automation processes to allow users to easily generate tables of cross sections (written to file) as well as presentation-style plots according to a user-defined

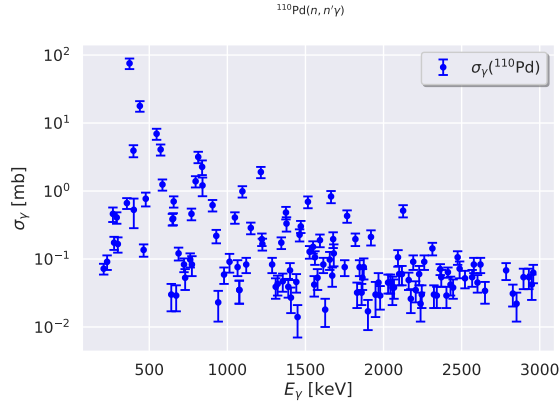


Figure 4: Absolute partial γ -ray cross sections for the $^{110}\text{Pd}(n, n'\gamma)$ reaction extracted from the Baghdad Atlas database using the Python Notebook automation methods.

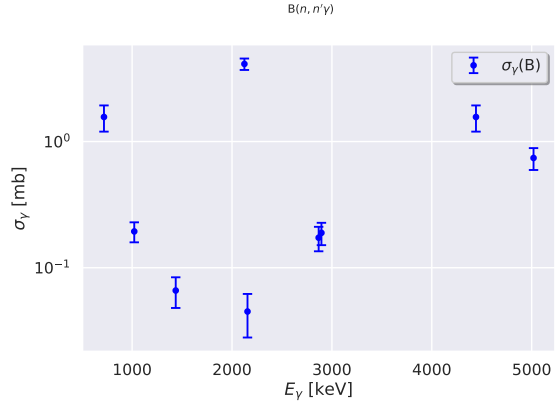


Figure 5: Absolute partial γ -ray cross sections for the $^{\text{nat}}\text{B}(n, n'\gamma)$ reaction extracted from the Baghdad Atlas database using the Python Notebook automation methods.

nucleus: *atomic mass*, *atomic number*, and *chemical symbol*. For example, in the case of the enriched isotope ^{110}Pd , we simply define: `Z = int(46)`, `A = int(110)`, and `Chem_symb = str('110Pd')` in the appropriate cell of the Notebook prior to execution of the cell to generate the plot of energy-dependent partial γ -ray cross sections in Fig. 4. For natural samples of elemental composition, the atomic mass is defined as $A = 0$. Thus, in the case of a natural boron sample, for example, we define: `Z = int(5)`, `A = int(0)`, and `Chem_symb = str('B')` to generate the plot shown in Fig. 5. The `CrossSection` class implemented in the Notebook that is used to generate these normalized data sets contains constants associated with the deduced flux-weighted average cross section for ^{56}Fe , $\langle\sigma_{\gamma 847}\rangle = 329.46 \pm 37.55$ mb (see Sect. 3). Adjustment of these class constants also provides users with the freedom to renormalize data sets according to different expectation values obtained from other neutron-data libraries or experimental measurements in a straightforward manner. Moreover, revisions to the adopted normalization cross section do not impact the source branching-ratio data stored on disk.

6. Summary and outlook

This first release of the Baghdad Atlas database is designed to serve the needs of the applications community. The energy levels, γ -ray energies and intensities are those stated in the Atlas [6] itself and have not, in general, been reconciled to match the adopted values in the ENSDF database [20], although state-of-the-art structure information has been used to identify γ -ray doublets (reported as unresolved doublets for now). Our intention is to issue periodic revisions where the γ -ray and level-scheme information for specific nuclei has been updated to match modern values in ENSDF [20], that can subsequently be used for more general dissemination to the wider-user community.

In addition to its immediate use to the applications community, the Baghdad Atlas can serve as a valuable resource to both the nuclear structure and reactions evaluations communities. Since (n, n') at fast-reactor neutron energies proceeds via both direct and compound processes it provides a non-selective insight into the properties of off-yrast levels over a far wider range of spins than thermal and epithermal neutron capture. This property of (n, n') has made it an attractive area of study to many research groups in the international nuclear science community. This is exemplified by the plethora of papers on

$^{56}\text{Fe}(n, n'\gamma)$ by groups from Russia [21], Los Alamos [22, 23], GELINA [24], and Dresden [25].

Lastly, we hope that this SQLite database will provide a useful tool for the reactions evaluation community by providing easy access to energy-integrated data to aid in the benchmarking process needed for the validation of Evaluated Nuclear Data File libraries.

Acknowledgments

This material is based upon work supported by the Department of Energy National Nuclear Security Administration under Awards No. DE-NA0003180 and No. DE-NA0000979. This work is also supported in part by the Lawrence Berkeley National Laboratory under Contract No. DE-AC02-05CH11231 for the US Nuclear Data Program. The authors would like to thank Dr. Andre Trkov for “saving” the Baghdad Atlas, in addition to Dr. Rick Firestone, Dr. Bradley Sleaford, and Dr. David Brown for helpful discussions and feedback.

References

- [1] Lee Bernstein, David Brown, Shamsuzzoha Basunia, Aaron Hurst, Toshihiko Kawano, John Kelley, Filip Kondev, Elizabeth McCutchan, Caroline Nesaraja, Rachel Slaybaugh, Alejandro Sonzogni, Nuclear data needs and capabilities for applications, White paper LLNL Report LLNL-CONF-676585 (2015).
URL <http://bang.berkeley.edu/events/ndnca/whitepaper>
- [2] Catherine Romano, Timothy Ault, Lee Bernstein, Rian Bahran, Patrick Talou, Brian Quiter, Sara Pozzi, Matt Devlin, Jason Burke, Todd Bredeweg, Elizabeth McCutchan, Sean Stave, Teresa Bailey, Susan Hogle, Christopher Chapman, Aaron Hurst, Noel Nelson, Fredrik Tovesson, Donald Hornback, Proceedings of the Nuclear Data Roadmapping and Enhancement Workshop (NDREW) for Nonproliferation, White paper ORNL/LTR-2018/510 (2018).
URL https://www.nndc.bnl.gov/nndcscr/documents/ndrew/NDREWProc_FINAL.pdf
- [3] Lee Bernstein, Catherine Romano, David Brown, Robert Casperson, Marie-Anne Descalle, Matthew Devlin, Chris Pickett, Brad Rearden, Cristiaan Vermeulen, Final Report for the Workshop for Applied Nuclear Data Activities (WANDA), White paper LLNL Report LLNL-PROC-769849 (2019).
URL <https://nucleardata.berkeley.edu/wanda/>
- [4] National Nuclear Data Center, Experimental Nuclear Reaction Data (EXFOR), <https://www.nndc.bnl.gov/exfor/>, online; accessed June 4, 2022.
- [5] National Nuclear Data Center, Experimental Unevaluated Nuclear Data List (XUNDL), <https://www.nndc.bnl.gov/ensdf/ensdf/xundl.jsp>, online; accessed June 4, 2022.
- [6] A. M. Demidov, L. I. Govor, Y. K. Cherepantsev, M. R. Ahmed, S. Al-Najjar, M. A. Al-Amili, N. Al-Assafi, N. Rammo, Atlas of Gamma-Ray Spectra from the Inelastic Scattering of Reactor Fast Neutrons, Moscow, Atomizdat, 1978 (1978).
- [7] Berkeley Nuclear Data Group, Atlas of Gamma-Ray Spectra from the Inelastic Scattering of Reactor Fast Neutrons, <https://nucleardata.berkeley.edu>, online; accessed June 4, 2022.
- [8] National Nuclear Data Center, Atlas of Gamma-Ray Spectra from the Inelastic Scattering of Reactor Fast Neutrons, <https://www.nndc.bnl.gov/lbnlatl.html>, online; accessed June 4, 2022.
- [9] M. R. Ahmed, K. I. Shakarchi, S. Al-Najjar, M. A. Al-Amili, L. I. Govor, A. M. Demidov, Investigation of gamma-ray spectra from the inelastic scattering of reactor fast neutrons, Nucl. Instrum. Methods 117 (1974) 533 (1974).
- [10] M. R. Ahmed, S. Al-Najjar, M. A. Al-Amili, N. Rammo, Y. S. Al-Shiraida, A. M. Demidov,

- L. I. Govor, Y. K. Cherepantsev, De-excitation of the $^{116,118,120,122,124}\text{Sn}$ levels from the inelastic scattering of reactor fast neutrons, Rep. IAE 846, preprint (1974).
- [11] L. Nichol, T. J. Kennet, Inelastic neutron scattering in the region $a = 11\text{--}40$, *Canad. J. Phys.* 50 (1972) 553 (1972).
- [12] D. A. Brown, M. B. Chadwick, R. Capote, A. C. Kahler, A. Trkov, M. W. Herman, A. A. Sonzogni, Y. Danon, A. D. Carlson, M. Dunn, D. L. Smith, G. M. Hale, G. Arbanas, R. Arcilla, C. R. Bates, B. Beck, B. Becker, F. Brown, R. J. Casperson, J. Conlin, D. E. Cullen, M. A. Descalle, R. Firestone, T. Gaines, K. H. Guber, A. I. Hawari, J. Holmes, T. D. Johnson, T. Kawano, B. C. Kiedrowski, A. J. Koning, S. Kopecky, L. Leal, J. P. Lestone, C. Lubitz, J. I. Marquez Damian, C. M. Mattoon, E. A. McCutchan, S. Mughabghab, P. Navratil, D. Neudecker, G. P. A. Nobre, G. Noguere, M. Paris, M. T. Pigni, A. J. Plompen, B. Pritychenko, V. G. Pronyaev, D. Roubtsov, D. Rochman, P. Romano, P. Schillebeeckx, S. Simakov, M. Sin, I. Sirakov, B. Sleaford, V. Sobes, E. S. Soukhovitskii, I. Stetcu, P. Talou, I. Thompson, S. van der Marck, L. Welser-Sherrell, D. Wiarda, M. White, J. L. Wormald, R. Q. Wright, M. Zerkle, G. Zerovnik, Y. Zhu, *Endf / b-viii.0: The 8 th major release of the nuclear reaction data library with cielo-project cross sections, new standards and thermal scattering data*, *Nucl.Data Sheets* 148 (2018) 1 (2018).
- [13] J. Huo, S. Huo, Y. Dong, Nuclear Data Sheets for $A = 56$, *Nucl. Data Sheets* 112 (2011) 1513 (2011).
- [14] SQLite3: an embedded SQL database engine, <https://www.sqlite.org/index.html>, online; accessed June 4, 2022.
- [15] GCC, the GNU Compiler Collection, <https://gcc.gnu.org>, online; accessed June 4, 2022.
- [16] Python, programming language, <https://www.python.org>, online; accessed June 4, 2022.
- [17] DB Browser for SQLite, <https://sqlitebrowser.org/>, online; accessed June 4, 2022.
- [18] SQLite Studio, <https://sqlitestudio.pl/index.rvt>, online; accessed June 4, 2022.
- [19] Jupyter, <https://jupyter.readthedocs.io/en/latest/install.html>, online; accessed June 4, 2022.
- [20] National Nuclear Data Center, Evaluated Nuclear Structure Data File (ENSDF), <https://www.nndc.bnl.gov/ensdf/>, online; accessed June 4, 2022.
- [21] A. M. Demidov, L. I. Govor, V. A. Kurki, I. V. Mikhailov, Employing $(n, n'\gamma)$ reactions to exclude nuclear levels erroneously introduced in other investigations: On the 3_1^- level in ^{56}Fe , *Yad.Fiz.* 67 (2004) 1908 (2004).
- [22] N. Fotiades, R. O. Nelson, M. Devlin, First 3^- excited state of ^{56}Fe , *Phys. Rev. C* 81 (2010) 037304 (2010).
- [23] N. Fotiades, G. D. Johns, R. O. Nelson, M. B. Chadwick, M. Devlin, M. S. Wilburn, P. G. Young, J. A. Becker, D. E. Archer, L. A. Bernstein, P. E. Garrett, C. A. McGrath, D. P. McNabb, W. Younes, Measurements and calculations of $^{238}\text{U}(n, xn\gamma)$ partial γ -ray cross sections, *Phys. Rev. C* 69 (2004) 024601 (2004).
- [24] A. Negret, C. Borcea, P. Dessagne, M. Kerveno, A. Olacel, A. J. M. Plompen, M. Stanoiu, Cross-section measurements for the $^{56}\text{Fe}(n, xn\gamma)$ reactions, *Phys. Rev. C* 90 (2014) 034602 (2014).
- [25] R. Beyer, R. Schwengner, R. Hannaske, A. R. Junghans, R. Massarczyk, M. Anders, D. Bemmmerer, A. Ferrari, A. Hartmann, T. Kogler, M. Roder, K. Schmidt, A. Wagner, Inelastic scattering of fast neutrons from excited states in ^{56}Fe , *Nucl. Phys. A* 927 (2014) 41 (2014).